



Contents lists available at ScienceDirect

## Chemical Engineering Science

journal homepage: [www.elsevier.com/locate/ces](http://www.elsevier.com/locate/ces)

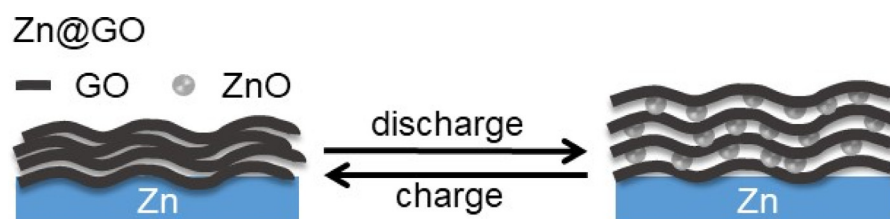
## Graphene oxide-modified zinc anode for rechargeable aqueous batteries

Zhubo Zhou<sup>a,1</sup>, Yamin Zhang<sup>a,1</sup>, Peng Chen<sup>a,b</sup>, Yutong Wu<sup>a</sup>, Haochen Yang<sup>a</sup>, Haoran Ding<sup>a,c</sup>, Yi Zhang<sup>a,d</sup>, Zhongzhen Wang<sup>a</sup>, Xu Du<sup>a</sup>, Nian Liu<sup>a,\*</sup><sup>a</sup> School of Chemical and Biomolecular Engineering, Georgia Institute of Technology, Atlanta, GA 30332, USA<sup>b</sup> School of Metallurgy, Northeastern University, Shenyang 110819, China<sup>c</sup> School of Chemical Engineering and Technology, Tianjin University, Tianjin 300072, China<sup>d</sup> College of Energy and Institute for Electrochemical Energy Storage, Nanjing Tech University, Nanjing, Jiangsu 211816, China

## HIGHLIGHTS

- Graphene oxide was uniformly coated onto the zinc anode.
- Graphene oxide coating suppresses the dissolution problem of zinc anodes.
- Graphene oxide alleviates the passivation problem of zinc anodes.
- Graphene oxide-modified Zn metal anode shows enhanced rechargeability.

## GRAPHICAL ABSTRACT



## ARTICLE INFO

## Article history:

Received 19 April 2018

Received in revised form 14 June 2018

Accepted 15 June 2018

Available online xxxxx

## Keywords:

Aqueous batteries  
Rechargeable  
Graphene oxide  
Passivation  
Dissolution  
Surface modification

## ABSTRACT

Li-based batteries are intrinsically unsafe because of their use of flammable organic electrolyte. Great efforts are being made to develop solid electrolytes or safer alternative battery chemistries, among which Zn-based batteries stand out for their high energy density and good compatibility with aqueous electrolyte. Theoretically, Zn-air batteries have very high volumetric energy density, which is ~85% of that of Li-S batteries. However, Zn anodes have poor cycling performance because of their passivation (insulating discharge product ZnO) and dissolution (soluble zinc species in alkaline electrolytes) problems.

In this work, we overcome these problems by modifying Zn anode with graphene oxide (Zn@GO) by a facile solution casting method. The GO layers on the Zn surface can deliver electrons across insulating ZnO, slow down the Zn intermediates from dissolving into the electrolyte, and thereby enhance the utilization and rechargeability of Zn anodes. As a result, the Zn@GO anode containing only 1.92 wt% GO showed improved cycling performance compared to that of the unmodified Zn mesh. The accumulated areal discharge capacity of the Zn@GO anode is 128% of that of the unmodified Zn mesh. The Zn@GO anode reported here can potentially be paired with oxygen cathode to form safe high-energy rechargeable batteries, and be used in large scale applications, ranging from electric vehicles, to grid-scale energy storage. The surface modification method reported here can also potentially be applied to other high-capacity electrodes that undergo passivation or dissolution issues.

© 2018 Elsevier Ltd. All rights reserved.

## 1. Introduction

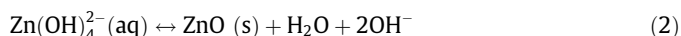
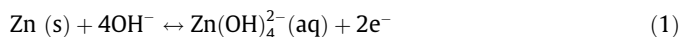
The depletion of fossil fuel and attention to environmental issues motivate tremendous research efforts on renewable energy (Obama, 2017). Batteries revolutionize transportation by powering zero-emission vehicles and could increase the utilization of

\* Corresponding author.

E-mail address: [nian.liu@chbe.gatech.edu](mailto:nian.liu@chbe.gatech.edu) (N. Liu).<sup>1</sup> These authors contributed equally to this work.

intermittent solar and wind electricity (Chu et al., 2017). Lithium-ion batteries are widely adopted in energy storage system (Lu et al., 2015; Sun et al., 2016; Wood et al., 2016; Zhang et al., 2017) due to their outstanding energy density and rechargeability (Zhang and Liu, 2017). However, the use of flammable organic electrolytes (Xu, 2014) arises safety concerns thus restricts the scale-up of Li-ion batteries. Aqueous rechargeable batteries are viewed as attractive alternatives to lithium-ion batteries, due to their low cost, low flammability, and good rate capability (Fu et al., 2017; Kim et al., 2014; Liang et al., 2017; Parker et al., 2017). Zinc is the most active metal that is stable with water. With two valence electrons and high density (7.1 g/cm<sup>3</sup>), Zn has three times the volumetric capacity of lithium metal. When paired with oxygen cathode, Zn-air batteries have almost the same energy density as lithium-sulfur batteries (Li et al., 2013; Li and Dai, 2014). Unlike Li-ion batteries, whose manufacturing requires dry room, Zn-based batteries can be manufactured in ambient air and are more tolerant to harsh operating environment and conditions.

One of the biggest challenges of Zn anodes is its rechargeability. Compared to conventional intercalation electrodes in lithium ion batteries, the solid-solute-solid transformation, as shown in Eqs. (1) and (2), of the Zn anodes brings certain challenges: (i) insulating discharge product ZnO passivates the surface of Zn and therefore will eventually terminate the discharging process; (ii) the insulating nature of ZnO makes it extremely hard for ZnO to convert back to metallic Zn; (iii) Zn inevitably dissolves into the electrolyte during the repeated discharging-charging process and thus lead to lose of active materials in the anode. As a result, the passivation and dissolution of Zn anodes lead to low utilization of Zn anodes and make it non-rechargeable (Fig. 1a). Typical redox reactions of Zn anode in alkaline aqueous electrolyte could be described as:



Herein, we solve the passivation and dissolution problems of Zn anodes through applying GO onto Zn mesh surface (Fig. 1b). GO is a layered material, which consists of hydrophilic oxygenated graphene sheets bearing oxygen functional groups on their basal planes and edges (Dikin et al., 2007). GO has been demonstrated to have ionic sieving capability. Ions that are smaller in size than the GO nanochannel can permeate in the GO layers, while larger ions will be blocked (Mi, 2014). In addition, GO could be partially reduced when soaked in alkaline solution (Fan et al., 2008) and facilitate the electron transport across ZnO (Supplementary Fig. S1). Therefore, our structure has the following advantages: (i) During cycling,  $\text{Zn(OH)}_4^{2-}$  will be blocked by the GO compared to  $\text{H}_2\text{O}$  and  $\text{OH}^-$ . Thus, the active material loss of anodes can be min-

imized. (ii) Zincate can form hydrogen bonds with oxygen-containing groups on the GO surface and thus has a good affinity with GO, which results in a relatively uniform distribution of zincate among GO layers during the reaction. Once the zincate reaches its solubility, it will decompose to ZnO, which will be encapsulated by GO. The GO encapsulation of ZnO can create the desirable environment for free transportation of electrons and therefore makes ZnO electrochemically active.

We chose to use Zn mesh as the anode instead of Zn foil because Zn mesh has relatively higher specific surface area with three-dimensional structure. The electrochemical performance of our anodes is tested using coin-type cells because they use minimum amount of electrolyte and resemble the practical operating condition. They are assembled in commercial CR2032 coin-type battery cases using NiOOH as the cathode.

## 2. Materials and methods

### 2.1. Materials

The following materials and chemicals are used in this work: water binder (MTI Corporation), graphite (Sigma-Aldrich), sulfuric acid ( $\text{H}_2\text{SO}_4$ , Fisher Scientific), Zn mesh (Dexmet Corporation), glass fiber (GE Healthcare, Whatman™ 10370003), commercial Ni-Zn AA batteries (PowerGenix), potassium permanganate ( $\text{KMnO}_4$ , Sigma-Aldrich), potassium hydroxide ( $\text{KOH}$ , Sigma-Aldrich), potassium fluoride ( $\text{KF}$ , Sigma-Aldrich), potassium carbonate ( $\text{K}_2\text{CO}_3$ , Sigma-Aldrich).

### 2.2. Methods

#### 2.2.1. Synthesis of GO powders

Modified Hummer method is utilized to produce aqueous GO solution (Marcano et al., 2010). A pretreatment was carried out to prevent the formation of inadequate oxidized graphite-core/GO-shell particles (Rashidi et al., 2017). The pretreated powder was placed in a beaker containing 120 ml concentrated  $\text{H}_2\text{SO}_4$  solution. Under stirring in ice bath, 15 g  $\text{KMnO}_4$  was added into the beaker. When the  $\text{KMnO}_4$  powder dissolved completely, the ice bath was removed, and the beaker was heated to 35 °C. After maintaining the mixture temperature at 35 °C for 45 min, 200 ml deionized water was added to the beaker drop by drop. The mixture was then heated to 98 °C and maintained at 98 °C for 15 min. Subsequently, another 700 ml deionized water was added to the mixture in order to decompose unreacted  $\text{KMnO}_4$  and insoluble  $\text{MnO}_2$ . The color of the mixture changed to bright-yellow. Subsequently, the GO was centrifuged (7000 rpm, 15 min) and redispersed in water for 5 times to remove ions. The resulting suspension was then subject to a 2 h sonication, followed by a 15-min centrifugation at 4000 rpm. The transparent supernatant was obtained as the GO aqueous solution (~1 g/L). This GO solution was then concentrated using hydrogel beads until a 2.0 g/L concentration was reached. Finally, GO powders were obtained through freeze-drying.

#### 2.2.2. Fabrication of GO-coated Zn anodes

GO/water binder slurry was prepared by mixing 2.1 mg GO powder, 2.4 mg water binder, and 160  $\mu\text{L}$  water in a glass vial under sonication for 60 min. The slurry was then stirred for 1 day at room temperature to ensure thorough mixing.

Zn mesh was cut into round disks with 1 cm diameter using a precision disc cutter and then weighed. After that, the GO slurry was applied onto the surface of the Zn mesh disks and dried for 20 min. To obtain a uniform GO-modified Zn surface, the GO slurry was applied one more time, especially the parts that have not yet been covered with GO. Finally, the GO-modified Zn mesh was dried at room temperature in air.

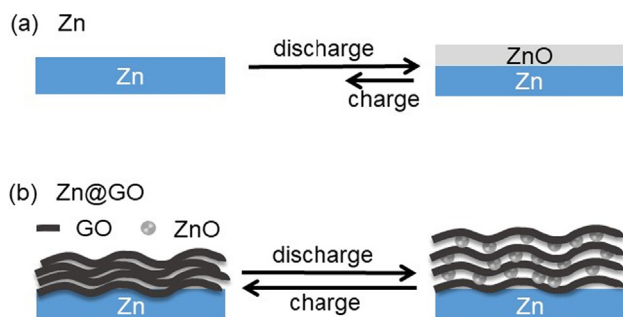
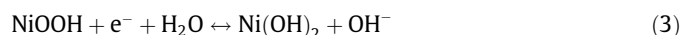


**Fig. 1.** Schematic of morphological changes of zinc electrodes during electrochemical cycling. (a) ZnO passivation layer leads to low utilization of the Zn mesh anode. (b) GO on Zn surface makes it possible for electrons to move freely across the insulating ZnO and slows down the dissolution of Zn species.

### 2.2.3. Preparation of Ni cathodes

To evaluate the electrochemical performance of GO-modified Zn anode, Ni cathodes harvested from commercial Ni–Zn AA batteries were used as the rechargeable cathode. Before cell assembly, Ni cathodes were electrochemically oxidized to 0.6 V vs HgO/Hg reference electrode in a beaker cell with 2 M KOH as the electrolyte, to completely turn Ni(OH)<sub>2</sub> to NiOOH. The reversible redox reaction of the cathode is:



### 2.2.4. Assembly of coin-type rechargeable Zn–Ni batteries

The coin-type batteries were assembled using CR2032 cases (MTI Corporation), the Zn mesh anodes or Zn@GO anodes (round disk, 1 cm diameter) and NiOOH cathodes with excess capacity. Glass fiber was used as the separator. 50  $\mu\text{L}$  electrolyte was added onto each separator. The aqueous electrolyte consists of 4 M KOH, 2 M KF and 2 M K<sub>2</sub>CO<sub>3</sub>. An MSK-110 M hydraulic sealing machine was used to seal the battery.

### 2.2.5. Materials characterization and electrochemical testing

X-ray photoelectron spectroscopy (XPS), X-ray diffraction (XRD), Scanning Electron Microscopy (SEM) and Transmission Electron Microscopy (TEM) at Institute for Electronics and Nanotechnology (IEN) were used to characterize the GO and anodes. The cycle life and capacity of our batteries were measured by using a LAND battery tester. All the cells were galvanostatically cycled between 1.5 V and 1.9 V at a constant current of 1 mA with 1 h limit. Electrochemical impedance spectroscopy (EIS) measurements were performed on a Bio-Logic instrument. The frequency range was between 100 kHz and 10 mHz. The amplitude of AC signal was 10 mV.

## 3. Results and discussion

As shown in Fig. 2a, we successfully synthesized high quality GO with nano thick GO layers. Then we applied GO slurry on Zn mesh (Fig. 2b). The comparison between Fig. 2c and f shows that GO has been coated onto the Zn mesh uniformly. By comparing

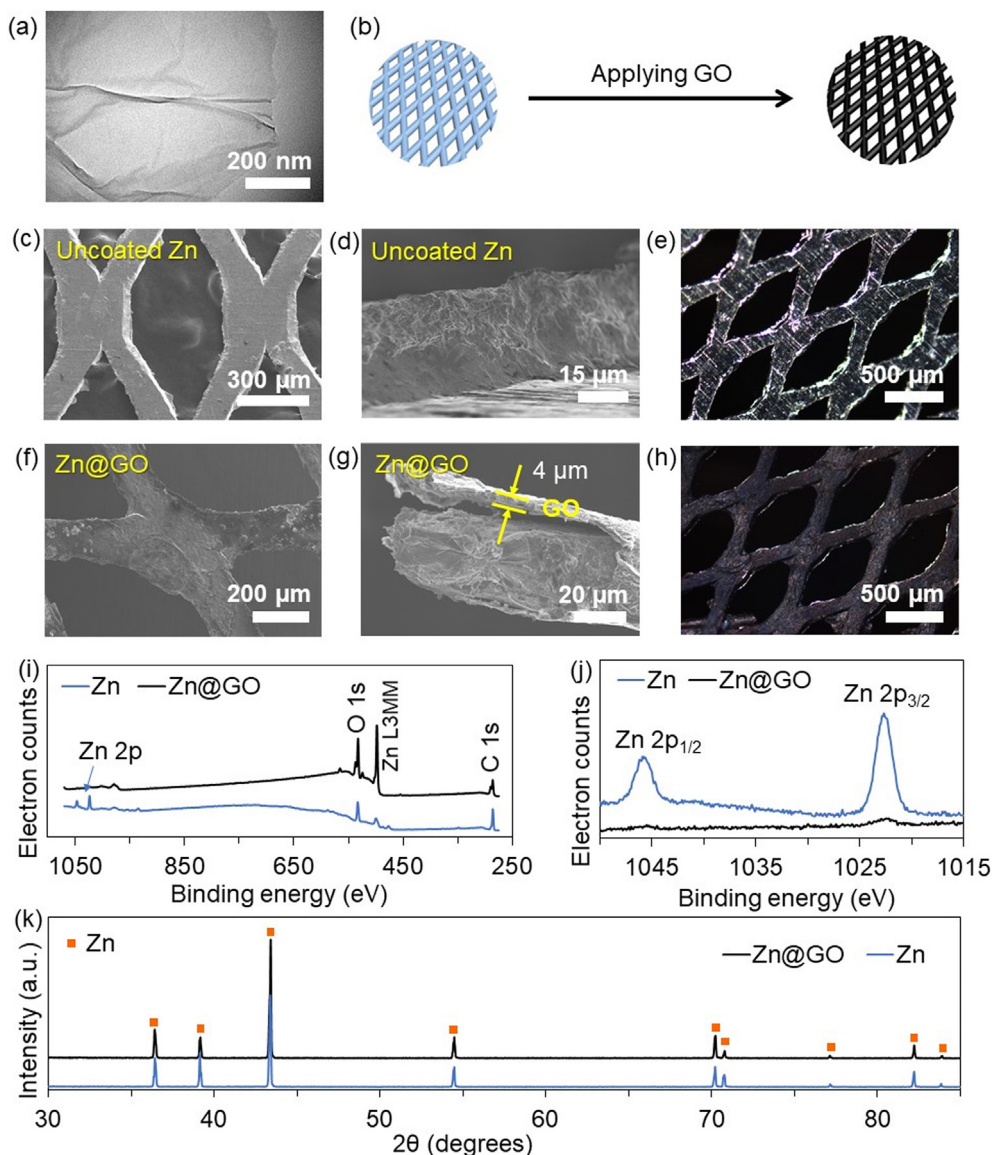


**Fig. 2.** Fabrication and characterization of anodes. (a) TEM image of GO. (b) Schematic of the fabrication process. (c) Top-view SEM image of Zn mesh. (d) Cross-section SEM image of Zn mesh. (e) Optical microscopy image of Zn mesh. (f) Top-view SEM image of GO modified Zn mesh. (g) Cross-section SEM image of GO modified Zn mesh. (h) Optical microscopy image of GO modified Zn mesh. (i) XPS survey of Zn mesh and GO modified Zn mesh. The C peak of Zn mesh is from the carbon tape under the Zn metal, which we used to fix the Zn mesh. (j) High-resolution Zn 2p spectra of Zn mesh and GO modified Zn mesh. (k) XRD results of Zn mesh and GO modified Zn mesh.



Fig. 2d and g, we can find that the GO coating is  $\sim 4 \mu\text{m}$  thick with a  $0.19 \text{ mg/cm}^2$  GO coating, which is 1.92 wt% of a Zn mesh. Under optical microscope, Zn mesh looks shiny (Fig. 2e), and after GO coating, it turns uniformly dark in color and rough in texture (Fig. 2h). The complete coverage of Zn by GO is supported by XPS results (Fig. 2i and j), where the Zn signal is barely detectable from Zn@GO. XRD patterns (Fig. 2k) of unmodified Zn and Zn@GO anodes show same ZnO peaks, which indicate the amorphous nature of GO.

To verify the function of GO coating, Zn anodes were assembled with NiOOH cathodes in coin-type cells, discharged and charged for 10 times, and opened for characterization. As shown in Fig. 3a and b, the structure of the unmodified Zn mesh anode collapsed after cycling. In contrast, the shape of the Zn@GO anode remained after cycling (Fig. 3c and d), which means that the GO coating has effectively stabilized the Zn anode. This is also an evidence that GO blocks zincates and encapsulates insulating discharged product ZnO (Fig. 3e), so electrons can be delivered across insulating ZnO. These morphological observations confirmed our hypothesis that thin and uniform GO coating could address the problems of Zn metal anode.

Conventionally, beaker cells are used to examine the electrochemical performance of Zn-based batteries. Yet the large amount of electrolyte (ZnO saturated KOH solution) required by beaker cells significantly decrease the overall specific energy. Also, zincates in the electrolyte can participate in the reaction and conceal the true performance of Zn electrodes. Hence, coin-type cells were chosen here to evaluate the performance of our GO-modified Zn anode in a way that resembles practical applications, as shown in Fig. 4a. The areal density of the Zn mesh we use is  $10.05 \text{ mg/cm}^2$ . If discharged in a primary cell, its theoretical capacity is  $8.24 \text{ mA h/cm}^2$ . In our rechargeability testing, we limit its discharge capacity to  $1.27 \text{ mA h/cm}^2$  by limiting its discharge time to 1 h. As shown in Fig. 4b, the battery assembled using Zn@GO anode with

$0.19 \text{ mg/cm}^2$  GO coating displayed its superiority over the one assembled using bare Zn mesh anode. At the 20th galvanostatic cycle, the reversible discharge areal capacity of the Zn@GO anode is  $\sim 118\%$  of that of the bare Zn anode. The accumulated discharge capacity of GO-modified Zn anode ( $61.5 \text{ mA h/cm}^2$ ) is 128% of that of bare Zn anode ( $47.9 \text{ mA h/cm}^2$ , Fig. 4c) for the first 200 galvanostatic cycles. The voltage in the charging step of the Zn@GO anode is slightly lower than that of bare Zn anode at the 20th galvanostatic cycle, which means that the Zn@GO anode has lower overpotential (Fig. 4d). We also tested the performance of Zn@GO anodes with lower and higher amount of GO coating, respectively. The effect of low amount of GO coating is not evident because GO is not enough to cover the Zn surface. High amount of GO coating makes the performance worse because thick GO hinders the contact of electrode and electrolyte, which hinders the electrochemical reaction (Supplementary Fig. S2).

Electrochemical impedance spectroscopy (EIS) was employed to investigate the influence of GO modification on the impedance. The Nyquist plots of the GO-coated and bare Zn anodes before and after 10 galvanostatic cycles (1 mA for 1 min per cycle) are shown in Fig. 4e. The initial charge-transfer resistance of GO-coated Zn anode is lower than that of the uncoated Zn anode. After cycling, the impedance of both anodes decreases, yet that of GO modified Zn anode is still smaller. For Zn@GO anode, the impedance decreased after cycling because GO was partially reduced in alkaline electrolyte. For Zn anode, the zincates disperse surrounding the surface of Zn after cycling, which decreased the charge-transfer resistance. These observations indicate that GO improves the electrochemical performance of the original Zn anode, which can be attributed to a uniform distribution of ZnO among GO layers during the electrochemical reactions. This extends the cycle life of Zn-based batteries by both creating a desirable environment for electrons to transport freely and slowing down the inevitable dissolution process of active anode materials.

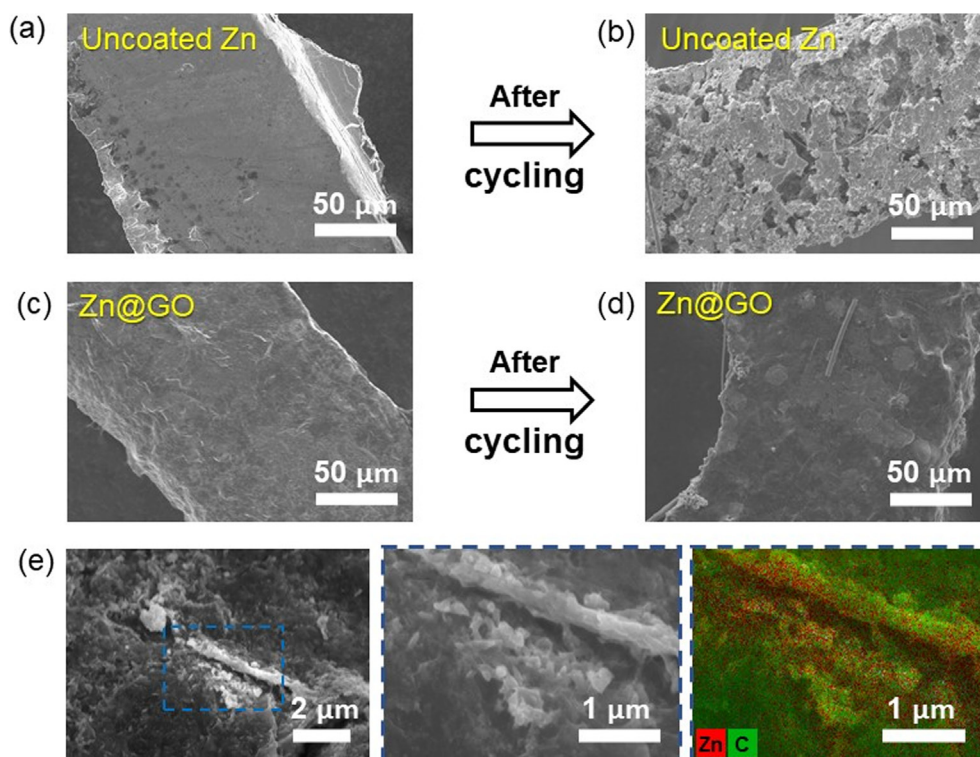
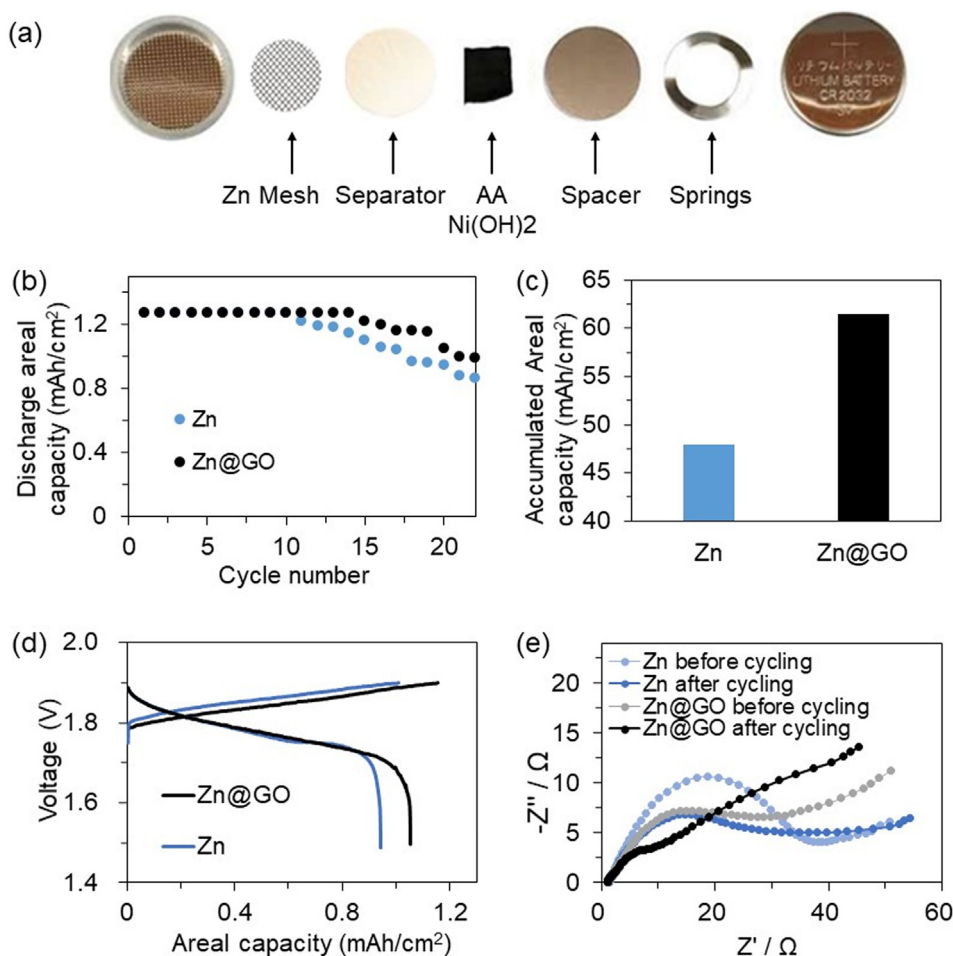


Fig. 3. Characterization of anodes before and after 10 galvanostatic cycles. (a) SEM image of unmodified Zn anode before cycling. (b) SEM image of unmodified Zn anode after cycling. (c) SEM image of Zn@GO anode before cycling. (d) SEM image of Zn@GO anode after cycling. (e) SEM images and EDS mapping of the Zn@GO anode after cycling.



**Fig. 4.** Electrochemical performance of anodes. (a) Optical picture of the coin cell assembly. (b) Discharge areal capacity for the first 22 galvanostatic cycles of bare and GO-modified Zn anodes. (c) Accumulated discharge areal capacity of bare and GO-modified Zn anodes for the first 200 galvanostatic cycles. Accumulated discharge areal capacity is calculated by adding the discharge areal capacity of all cycles together. (d) Voltage profiles of the 20th galvanostatic cycle of bare and GO-modified Zn anodes. (e) Nyquist plots of the bare and GO-modified Zn anodes before and after cycling.

#### 4. Conclusions

We have reported a GO-modified Zn anode to solve the passivation and dissolution problems of Zn anodes, and extend the cycle life of Zn-based batteries. The Zn surface is modified by applying GO slurry onto Zn mesh uniformly. The GO layers on Zn surface allow electrons to move freely across the insulating ZnO and reduce the dissolution rate of Zn intermediate species. As a result, a small amount of GO (1.92 wt%) on the Zn anode surface can significantly reduce the electrochemical impedance, and improve its life-time accumulated capacity by 28%. This GO modification approach is expected to be applicable to other battery electrodes as well.

#### Acknowledgment

This work was performed in part at the Georgia Tech Institute for Electronics and Nanotechnology, a member of the National Nanotechnology Coordinated Infrastructure, which is supported by the National Science Foundation (Grant ECCS-1542174). Nian Liu acknowledges support from faculty startup funds from the Georgia Institute of Technology. The authors thank Prof. Sankar Nair and Prof. Yulin Deng for helpful discussions on the synthesis of graphene oxide. Dexmet Corporation is acknowledged for providing Zn MicroGrid® Metals.

#### Appendix A. Supplementary material

Supplementary data associated with this article can be found, in the online version, at <https://doi.org/10.1016/j.ces.2018.06.048>.

#### References

- Chu, S., Cui, Y., Liu, N., 2017. The path towards sustainable energy. *Nat. Mater.* 16, 16–22. <https://doi.org/10.1038/nmat4834>.
- Dikin, D.A., Stankovich, S., Zimney, E.J., Piner, R.D., Dommett, G.H.B., Evmenenko, G., Nguyen, S.T., Ruoff, R.S., 2007. Preparation and characterization of graphene oxide paper. *Nature* 448, 457–460. <https://doi.org/10.1038/nature06016>.
- Fan, X., Peng, W., Li, Y., Li, X., Wang, S., Zhang, G., Zhang, F., 2008. Deoxygenation of exfoliated graphite oxide under alkaline conditions: a green route to graphene preparation. *Adv. Mater.* 20, 4490–4493. <https://doi.org/10.1002/adma.200801306>.
- Fu, J., Cano, Z.P., Park, M.G., Yu, A., Fowler, M., Chen, Z., 2017. Electrically rechargeable zinc-air batteries: progress, challenges, and perspectives. *Adv. Mater.* 29, 1604685. <https://doi.org/10.1002/adma.201604685>.
- Kim, H., Hong, J., Park, K.Y., Kim, H., Kim, S.W., Kang, K., 2014. Aqueous rechargeable Li and Na ion batteries. *Chem. Rev.* 114, 11788–11827. <https://doi.org/10.1021/cr500232y>.
- Li, Y., Dai, H., 2014. Recent advances in zinc-air batteries. *Chem. Soc. Rev.* 43, 5257–5275. <https://doi.org/10.1039/C4CS00015C>.
- Li, Y., Gong, M., Liang, Y., Feng, J., Kim, J.E., Wang, H., Hong, G., Zhang, B., Dai, H., 2013. Advanced zinc-air batteries based on high-performance hybrid electrocatalysts. *Nat. Commun.* 4, 1805–1807. <https://doi.org/10.1038/ncomms2812>.
- Liang, Y., Jing, Y., Gheytni, S., Lee, K.Y., Liu, P., Facchetti, A., Yao, Y., 2017. Universal quinone electrodes for long cycle life aqueous rechargeable batteries. *Nat. Mater.* 16, 841–848. <https://doi.org/10.1038/nmat4919>.

- Lu, Z., Liu, N., Lee, H.-W., Zhao, J., Li, W., Li, Y., Cui, Y., 2015. Nonfilling carbon coating of porous silicon micrometer-sized particles for high-performance lithium battery anodes. *ACS Nano* 9, 2540–2547. <https://doi.org/10.1021/nn505410q>.
- Marcano, D.C., Kosynkin, D.V., Berlin, J.M., Sinitskii, A., Sun, Z.Z., Slesarev, A., Alemany, L.B., Lu, W., Tour, J.M., 2010. Improved synthesis of graphene oxide. *ACS Nano* 4, 4806–4814. <https://doi.org/10.1021/nn1006368>.
- Mi, B., 2014. Graphene oxide membranes for ionic and molecular sieving. *Science* 80 (343), 740–742. <https://doi.org/10.1126/science.1250247>.
- Obama, B., 2017. The irreversible momentum of clean energy. *Science* 80 (355), 126–129. <https://doi.org/10.1126/science.aam6284>.
- Parker, J.F., Chervin, C.N., Pala, I.R., Machler, M., Burz, M.F., Long, J.W., Rolison, D.R., 2017. Rechargeable nickel–3D zinc batteries: an energy-dense, safer alternative to lithium-ion. *Science* 80 (356), 415–418. <https://doi.org/10.1126/science.aak9991>.
- Rashidi, F., Kevlich, N.S., Sinquefeld, S.A., Shofner, M.L., Nair, S., 2017. Graphene oxide membranes in extreme operating environments: concentration of kraft black liquor by lignin retention. *ACS Sustain. Chem. Eng.* 5, 1002–1009. <https://doi.org/10.1021/acssuschemeng.6b02321>.
- Sun, Y., Liu, N., Cui, Y., 2016. Promises and challenges of nanomaterials for lithium-based rechargeable batteries. *Nat. Energy* 1, 16071. <https://doi.org/10.1038/nenergy.2016.71>.
- Wood, K.N., Kazyak, E., Chadwick, A.F., Chen, K.H., Zhang, J.G., Thornton, K., Dasgupta, N.P., 2016. Dendrites and pits: untangling the complex behavior of lithium metal anodes through operando video microscopy. *ACS Cent. Sci.* 2, 790–801. <https://doi.org/10.1021/acscentsci.6b00260>.
- Xu, K., 2014. Electrolytes and interphases in Li-Ion batteries and beyond. *Chem. Rev.* 114, 11503–11618. <https://doi.org/10.1021/cr500003w>.
- Zhang, H., Huang, X., Noonan, O., Zhou, L., Yu, C., 2017. Tailored yolk-shell Sn@C nanoboxes for high-performance lithium storage. *Adv. Funct. Mater.* 27, 1606023. <https://doi.org/10.1002/adfm.201606023>.
- Zhang, Y., Liu, N., 2017. Nanostructured electrode materials for high-energy rechargeable Li, Na and Zn batteries. *Chem. Mater.* 29, 9589–9604. <https://doi.org/10.1021/acs.chemmater.7b03839>.